Mechanism and Selectivity of Bioinspired Cinchona Alkaloid Derivatives Catalyzed Asymmetric Olefin Isomerization: A Computational Study

ARTICLE *in* JOURNAL OF THE AMERICAN CHEMICAL SOCIETY · MAY 2013

Impact Factor: 12.11 · DOI: 10.1021/ja309133z · Source: PubMed

6 AUTHORS, INCLUDING:

Xiaosong Xue
Nankai University
21 PUBLICATIONS **250** CITATIONS
SEE PROFILE

Xin Li
Northwestern Polytechnical University
86 PUBLICATIONS **886** CITATIONS
SEE PROFILE

Chen Yang
Nankai University
8 PUBLICATIONS **97** CITATIONS
SEE PROFILE

JACS
JOURNAL OF THE AMERICAN CHEMICAL SOCIETY
Article
pubs.acs.org/JACS

Mechanism and Selectivity of Bioinspired Cinchona Alkaloid Derivatives Catalyzed Asymmetric Olefin Isomerization: A Computational Study

Xiao-Song Xue,[†,§] Xin Li,[†] Ao Yu,*[,‡] Chen Yang,[†] Chan Song,[‡] and Jin-Pei Cheng*[,†]

[†]State Key Laboratory of Elemento-Organic Chemistry, [§]Computational Center of Molecular Science, and [‡]Central Laboratory, College of Chemistry, Nankai University, Tianjin 300071, China

Supporting Information

ABSTRACT: Asymmetric olefin isomerization of β,γ- to α,β-unsaturated butenolides catalyzed by novel cinchona alkaloid derivatives was investigated in-depth using density functional theory (M05-2x and B2PLYP-D). Three possible mechanistic scenarios, differing in the binding modes of the substrate to the catalyst, have been evaluated. Computations revealed that both the protonated quinuclidine and the 6′-OH of catalysts may act as the proton donor in the stereocontrolling step. Variation of the catalytic activity and enantioselectivity by tuning the electronic effect of catalyst was well reproduced computationally. It suggested that, for certain acid−base bifunctional chiral catalysts, the acid−base active sites of catalysts may interconvert and give new catalyst varieties of higher activity and selectivity. In addition, the noncovalent interactions in the stereocontrolling transition-state structures were identified, and their strength was quantitatively estimated. The weak nonconventional C−H···O hydrogen-bonding interactions were found to be crucial to inducing the enantioselectivity of the cinchona alkaloid derivatives catalyzed asymmetric olefin isomerization. The computational results provided further theoretical evidence that the rate-limiting step of this bioinspired organocatalytic olefin isomerization is inconsistent with that of the enzyme catalyzed olefin isomerization.

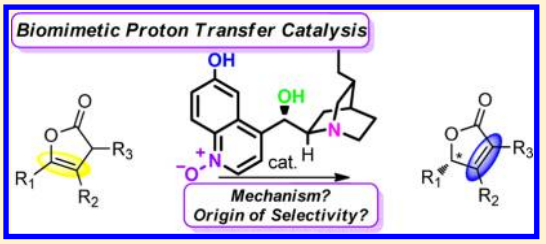

1. INTRODUCTION

The enzyme-mediated olefin isomerization, such as the Δ^5-3-ketosteroid isomerase (**KSI**) catalyzed isomerization of Δ^5-3-ketosteroids to the conjugated Δ^4-3-ketosteroids (Scheme 1A), is a common and important class of chemical reactions in biology.[1] Enzymes, as the nature's catalyst, have been a great source of inspiration for the development of new catalytic processes. By examining the chemical building blocks and the modes of substrate activation in biosynthetic pathways, considerable insights can be obtained and then similar transformations could be developed.[2] Subsequently, an explosive growth in the field of asymmetric organocatalysis with an impressive amount of new catalysts and their applications in various reaction types has been witnessed in the past decade.[3] Despite the great success achieved in asymmetric organocatalysis, the enantioselective olefin isomerization catalyzed by chiral organic small molecules remains an unusual challenge.[4]

Most recently, as inspired by nature's **KSI**, Deng and coworkers realized a general and highly enantioselective olefin isomerization via biomimetic proton-transfer catalysis with a novel cinchona alkaloid derived catalyst **QD-1a** (Scheme 1B).[5] The strategy of "electronic tuning of the catalyst"[6] was successfully applied to improve catalytic activity and selectivity. Ingeniously oxidizing the quinoline ring N of 6′-OH cinchona alkaloid (**QD-1b**) into its N-oxide analogue (**QD-1a**) achieved a significant enhancement of catalytic activity and selectivity (Scheme 1B). It was reported that the catalyst **QD-1a** could catalyze a broad range of β,γ-butenolides to yield α,β-unsaturated butenolides with excellent yields and enantioselectivities.[5] The γ-substituted α,β-unsaturated butenolides are a common structural motif in a broad array of natural products,[7] and they are versatile chiral building blocks in asymmetric synthesis.[8] Therefore, substantial attention has been paid to develop efficient methods for optically active γ-alkyl α,β-unsaturated butenolides synthesis.[9] Deng's work not only provided a valuable method for the asymmetric synthesis of chiral α,β-unsaturated butenolides but also demonstrated an excellent example of mimicking enzymatic catalysis with artificial organic small molecule structures, one of the most fascinating and provocative challenges presented by Nature.

Some key issues of the bioinspired asymmetric organocatalytic olefin isomerization remain obscure, however. First, though the cinchona alkaloids were proposed to be the **KSI** mimic, they have different rate-limiting steps. Deng's preliminary kinetic studies suggested that the protonation step be the rate-limiting step of the organocatalytic asymmetric olefin isomerization,[5] whereas the **KSI** catalyzed olefin isomerization features a rate-limiting deprotonation.[1a] Second, the preferred binding mode between the substrate and the catalyst in the stereocontrolling transition-state structure remains elusive. Whether the protonated quinuclidine, or the 6′-OH group of catalyst, acts as the proton donor in the

Received: September 19, 2012
Published: May 3, 2013

   dx.doi.org/10.1021/ja309133z | J. Am. Chem. Soc. 2013, 135, 7462−7473

Scheme 1. Enzyme (KSI) and Organic Small Molecules Catalyzed Olefin Isomerization via Proton Shift Processes

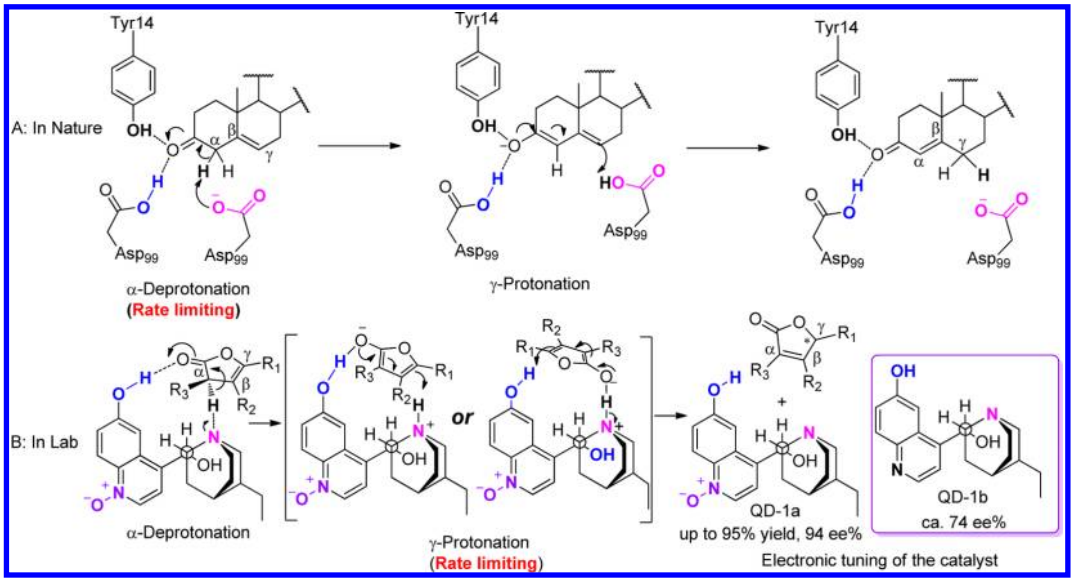

stereocontrolling step, still remains an open question. Third, the origin of asymmetric induction in the cinchona alkaloids catalyzed olefin isomerization is not yet known, though it is of great importance for understanding the reaction and for developing new reactions. Finally, although the strategy of "electronic tuning of the catalyst" has been nicely applied to optimize the catalytic activity and selectivity, the underlying reasons is not very clear.

Quantum mechanical investigations on proline catalyzed asymmetric aldol reactions featured the beginning of theoretical mechanism study of organocatalysis.[10] From then on, a great number of important organocatalytic systems has been successfully investigated with this powerful tool,[11] which has demonstrated that accurate quantum chemical calculations can provide valuable insights into the origin of the activity and selectivity of organocatalytic process.[12] Due to commercial availability and facile modification, cinchona alkaloids and their derivatives have been extensively used as catalysts in asymmetric synthesis.[13−16] Though the development of cinchona-derived compounds catalyzed reactions has emerged as a frontier of organocatalysis, computational mechanistic studies on these systems have received very limited attention.[12b,17] Owing to the high importance of this biomimetic asymmetric proton-transfer catalysis, we have conducted, as part of our continuing efforts in mechanism study of asymmetric organocatalysis,[18] an in-depth computational investigation of the novel cinchona alkaloid derivatives promoted olefin isomerization of butenolides.

In the present study, we first investigated various possible mechanistic scenarios that differ in catalytic modes. Calculation revealed that both the protonated quinuclidine and the 6′-OH of catalysts may function as the proton donor in the stereocontrolling step. Differing from previous mechanistic hypothesis,[5] it is the 6′-OH in this case that acts as the proton donor in the most favored catalytic mode of catalyst **QD-1a**. In all three mechanistic possibilities, γ-protonation was predicted to be the rate-limiting step of the **QD-1a** catalyzed reaction, which provided theoretical evidence that the rate-limiting step of this organocatalytic olefin isomerization differs from that of the enzyme catalyzed olefin isomerization. Next, we explored the origin of selectivity for this eye-catching transformation. An analysis of the electron density and their reduced density gradient (RDG) isosurface[19] of the stereocontrolling transition state structures revealed that the weak nonconventional hydrogen bonds (C−H···O)[20,21] play a crucial role in inducing selectivity. Finally, the electronic effect of the catalyst on the catalytic activity and enantioselectivity was analyzed. It was found that tuning the electronic effect of the catalyst altered the most favored catalytic mode. Contrasted with **QD-1a**, the most favored catalytic mode for **QD-1b** uses the protonated quinuclidine as the proton donor in the stereocontrolling step. The present study would add new insight into the current understanding of electronic effect of the catalysts[6a,b] and may hold general implication for cinchona alkaloids and other acid−base bifunctional chiral catalysts catalyzed reactions.[22]

2. COMPUTATIONAL METHODS

The recently developed M05-2x functional,[23] together with the standard 6-31+G(d) basis set, were used for optimizing the geometry of all the minima and transition states (**TS**) in solution. Houk and coworkers reported very good agreement between the M05-2x functional predictions and experimental observation for the cinchona alkaloid catalyzed rearrangement of allylic trichloroacetimidate.[17c] The new SMD solvation model was used to account for the effects of dichloromethane (DCM) environment.[24] Dielectric constant of 8.93 was used for DCM. In addition, all the optimized structures were confirmed by frequency calculations to be either minima or transition states using the same level of theory. Single point energy calculations were performed at the M05-2x/6-311+G(2d,p) and B2PLYP-D/6-31+G(d,p) level with the M05-2x/6-31+G(d)(SMD) structures. The B2PLYP-D is double-hybrid density functional with long-range dispersion correction.[25] All calculations were carried out with the GAUSSIAN 09 packages.[26] All energetics reported throughout the text are in kcal/mol, and the bond lengths are in angstroms (Å). Structures were generated using CYLview and VMD.[27]

3. RESULTS AND DISCUSSION

The catalyst **QD-1a** catalyzed isomerization of γ-methyl β,γ-butenolide (**R1**) to γ-methyl α,β-butenolide (**P1**) (Scheme 2) was first used as the model reaction to explore the details of the reaction mechanism and the origin of enantioselectivity. Then, the catalyst **QD-1b** catalyzed same isomerization reaction was

dx.doi.org/10.1021/ja309133z | J. Am. Chem. Soc. 2013, 135, 7462−7473

Scheme 2. Isomerization of γ-Methyl β,γ-Butenolide (R1) to γ-Methyl α,β-Butenolide (P1) Catalyzed by the Novel Cinchona Alkaloid Derivative QD-1a

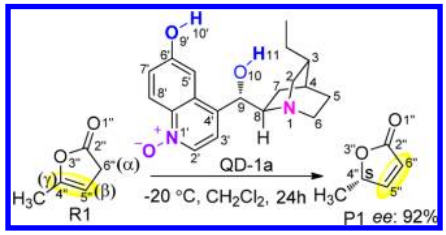

used to investigate the electronic effect of the catalyst on the catalytic mode, activity, and enantioselectivity.

On the basis of the previous experimental and computational studies of the cinchona alkaloids catalyzed reactions,[14d,17] the conformation space of catalyst **QD-1a** and transition states were studied. The lowest energy anti-open conformation of catalyst was considered in the present study.[28]

Mechanism of QD-1a Catalyzed Reaction. The proposed catalytic mechanism for the **QD-1a** catalyzed olefin isomerization of butenolides consists of two processes: the deprotonation of α-carbon of substrate **R1** and the subsequent protonation of γ-carbon in the same substrate molecule.[5] Considering different binding modes between the substrate and catalyst, at least three possible mechanistic scenarios can be envisioned. In Scenario I, the substrate **R1** binds to catalyst **QD-1a** by hydrogen-bonding interaction between the carbonyl oxygen of **R1** and the 6′-OH of **QD-1a**, and the α-deprotonation and γ-protonation are achieved with the quinuclidine nitrogen and the protonated quinuclidine, respectively. In Scenario II, the substrate **R1** binds to catalyst **QD-1a** by hydrogen-bonding interaction between the carbonyl oxygen of **R1** and the 9-OH of **QD-1a**. The deprotonation and protonation are similarly achieved as in Scenario I. In Scenario III, the substrate **R1** binds to the protonated quinuclidine of **QD-1a** by hydrogen-bonding interaction. The γ-protonation is achieved with the 6′-OH of catalyst **QD-1a**. The M05-2x/6-31+G(d)(SMD) calculated results of these mechanistic scenarios that lead to the experimentally observed major *s*-product are given in Figures 1−3 (for the *r*-product, see Figures S9−S11).

*Scenario I of **QD-1a** Catalyzed Reaction.* The first step in the mechanistic Scenario I of **QD-1a** catalyzed reaction is the coordination of the substrate **R1** with catalyst **QD-1a** by forming the hydrogen bond between the carbonyl oxygen (O1″) of **R1** and the 6′-OH of **QD-1a** (Figure 1). This complexation process, generating **CP1a**, is endergonic by 1.3 kcal/mol due to the entropy penalty for bringing two molecules together.[29] The distance of the hydrogen bond between H10′ and O1″ is 1.851 Å in **CP1a**. Deprotonation of the α-proton (H7″) of **R1** proceeds via **TS1a**, leading to intermediate **CP2a** with a barrier of 14.4 kcal/mol in free energy. During the deprotonation process, negative charge is gradually developed on the O1″ atom of **R1**. As a result, the interaction between the 6′-OH of **QD-1a** and the carbonyl oxygen of **R1** is strengthened, as demonstrated by the H10′···O1″ distance shortening from 1.851 Å in **CP1a** to 1.768 Å in **TS1a** and 1.614 Å in **CP2a**. The **CP2a** is 6.5 kcal/mol downhill from **TS1a**.

Protonation of the γ-carbon (C4″) by the protonated quinuclidine occurs via **TS2a(s)** with a barrier of 10.6 kcal/mol in free energy. In contrast to the deprotonation process, the hydrogen bonding interaction between the O1″ and the 6′-OH is weakened during protonation due to the gradually decreased negative charges on the O1″ atom. The H10′···O1″ distance is lengthened from 1.614 Å in **CP2a** to 1.707 Å in

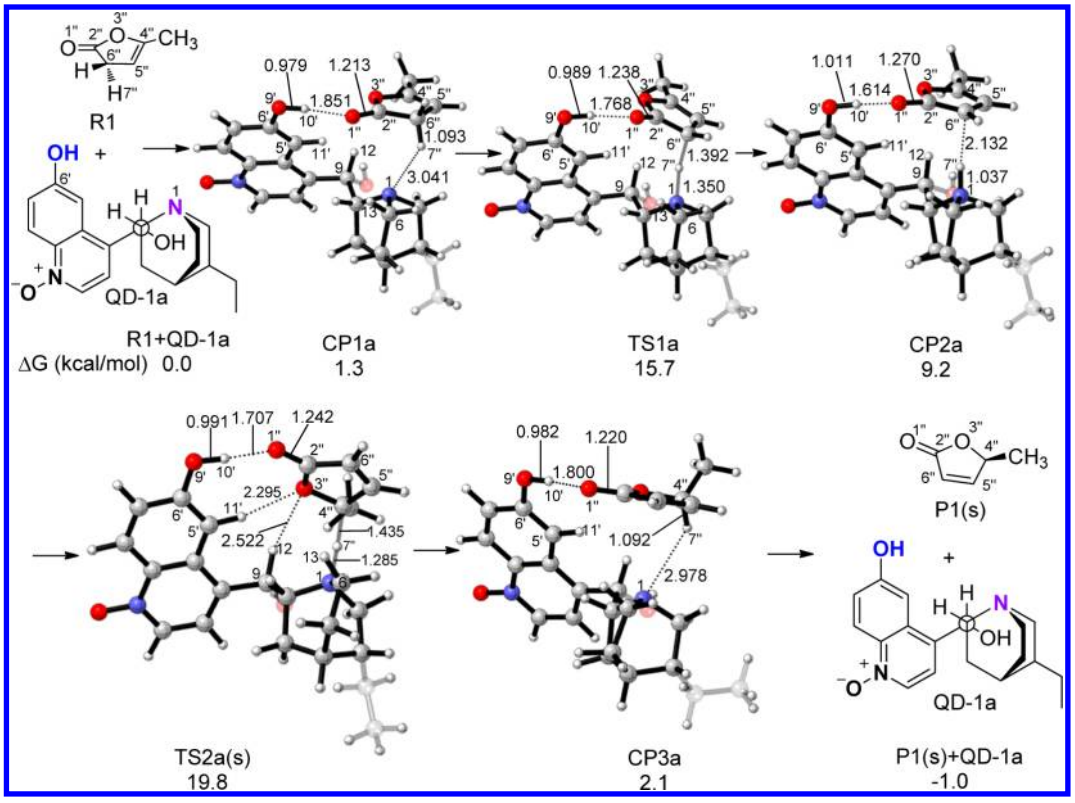

Figure 1. Energies and optimized geometries in Scenario I for the **QD-1a** catalyzed isomerization calculated with M05-2x/6-31+G(d)(SMD).

dx.doi.org/10.1021/ja309133z | J. Am. Chem. Soc. 2013, 135, 7462−7473

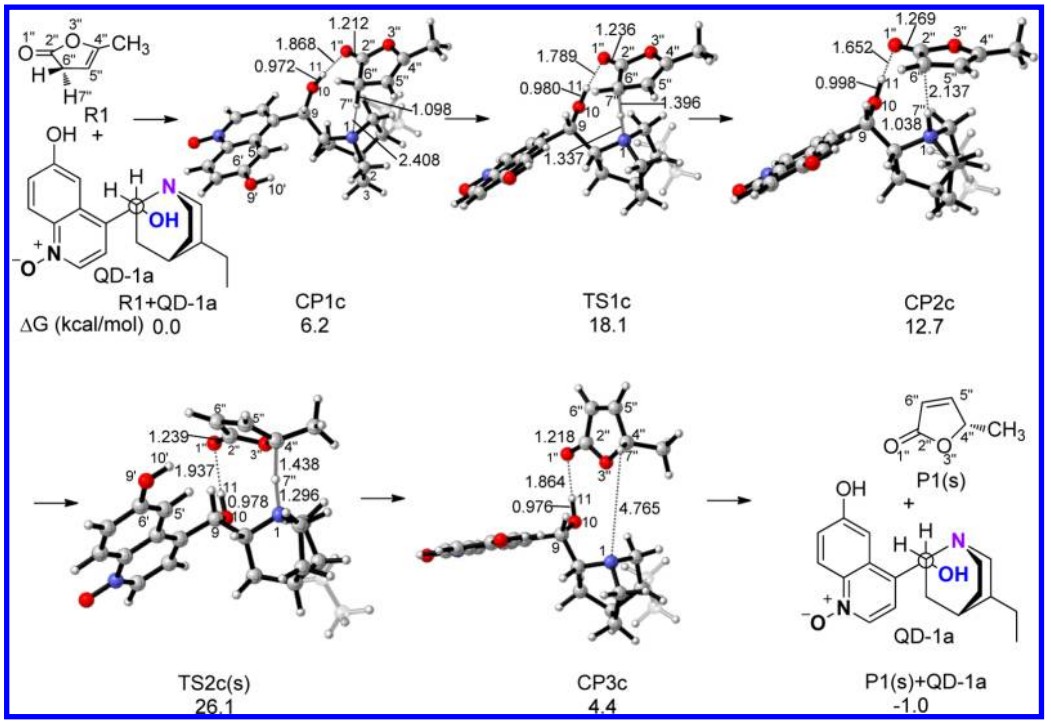

Figure 2. Energies and optimized geometries in Scenario II for the **QD-1a** catalyzed isomerization calculated with M05-2x/6-31+G(d)(SMD).

TS2a(s) and 1.800 Å in **CP3a**. The dissociation of **CP3a** leads to the release of the product. Reviewing the Scenario I of the **QD-1a** catalyzed reaction, the γ-protonation is the rate-limiting step, which requires an overall activation free energy of 19.8 kcal/mol in **DCM**.

*Scenario II of **QD-1a** Catalyzed Reaction.* Previous experiments and calculations also showed that the 9-OH group of cinchona alkaloids played an important role in some asymmetric catalytic reactions by hydrogen bonding with substrates.[13b,17c,d,30] Thus, it is reasonable to investigate the catalytic activity of 9-OH in **QD-1a**. In Scenario II, the substrate **R1** binds to the catalyst via a hydrogen bonding interaction between the carbonyl oxygen (O1″) of **R1** and the 9-OH group of **QD-1a** (Figure 2). **CP1c** is energetically 4.9 kcal/mol less stable than **CP1a**. The hydrogen-bond distance between H11 and O1″ is 1.868 Å in **CP1c**, which is 0.017 Å longer than that in **CP1a**. This is consistent with the fact that the 9-OH group is a weaker proton donor than 6′-OH due to its lower acidity. The subsequent α-deprotonation proceeds via **TS1c** with a barrier of 11.9 kcal/mol. Similarly, the hydrogen-bonding interaction between O1″ and H11 is strengthened as the H7″ of **R1** is transferring to the N1 of **QD-1a**. The calculation showed that γ-protonation is the rate-limiting step in Scenario II, requiring an overall activation free energy of 26.1 kcal/mol, which is 6.3 kcal/mol higher than that in Scenario I. It is consistent with the experimental observation that the activity of the 9-OH cinchona alkaloid catalyzed olefin isomerization is significantly lower than that of the 6′-OH cinchona alkaloid.[5]

*Scenario III of **QD-1a** Catalyzed Reaction.* Deng and co-worker proposed that the 6′-OH of **QD-1a** might also act as proton donor in the stereocontrolling step.[5] Our calculation showed, however, that the sum of free energies of the separated butenolide anion and protonated **QD-1a** is 24.9 kcal/mol higher than that of **R1** and **QD-1a** (Scheme 3).[31] Because the γ-protonation via **TS2a(s)** needs only 19.8 kcal/mol to pass

Scheme 3. Free Energies Required for the Dissociation and γ-Protonation of CP2a Calculated with M05-2x/6-31+G(d)(SMD)

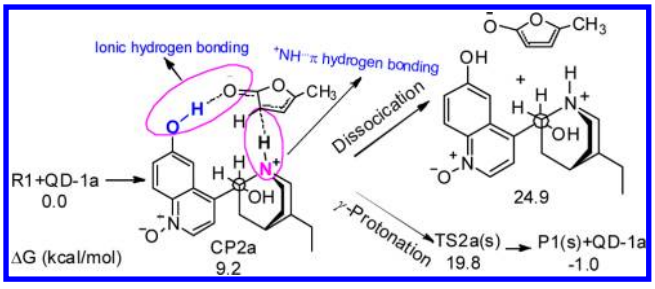

through, it should be not favorable for intermediate **CP2a** to dissociate into the protonated **QD-1a** and butenolide ion and then finish the γ-protonation with 6′-OH as the proton donor. This suggests that there should be other complexed form besides **CP2a** to bind the catalyst and substrate together. These dissociation and protonation steps were further validated by the additional high level M05-2x/6-311+G(2d,p)//M05-2x/6-31+G(d)(SMD) and B2PLYP-D/6-31+G(d,p)//M05-2x/6-31+G(d)(SMD) calculations (see Scheme S1). Two possible reasons might account for the high-energy barrier required for dissociation of intermediate **CP2a** into the protonated **QD-1a** and butenolide ion. One is due to the high instability of butenolide ion in less polar DCM, and the other should be related to that the dissociation requests breaking a $^{+}$N−H···π hydrogen bond and an ionic hydrogen bond (O−H···O^{-}), whose strength has been shown to be 5−35 kcal/mol, up to one-third of the strength of covalent bonds.[32]

On the other hand, it was reported that a very small amount of the zwitterionic form (**6HQ′**) of 6-hydroxyquinoline (**6HQ**) could coexist with the parent **6HQ** (Scheme 4) under neutral conditions based on a meticulous analysis of their absorption spectra.[33] Moreover, it was also shown that oxidization of **6HQ**

dx.doi.org/10.1021/ja309133z | J. Am. Chem. Soc. 2013, 135, 7462−7473

Scheme 4. Possible Tautomeric Form of 6HQ, 6HQNO, QD-1a, and QD-1b[35]

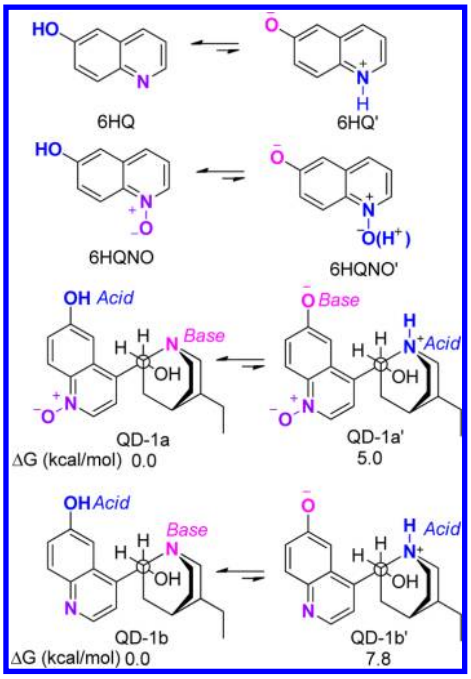

into its N-oxide form (**6HQNO**) significantly enhanced its acidity and thus increased the propensity of donating the proton of the 6-hydroxy group.[34] Based on these observations, it can be expected that the zwitterion ion **QD-1a′** may also coexist with its neutral N-oxide form **QD-1a**. The present calculation has verified the hypothesis that **QD-1a** is easier to intercovert into its zwitterion ion **QD-1a′** than **QD-1b**, although the amount of **QD-1a′** might be low (cf. the difference of relative free energies between **QD-1a**/**QD-1a′** and **QD-1b**/**QD-1b′** in Scheme 4).

In order to find some unambiguous support from experiment for the species suggested by calculation, we have deliberately synthesized **QD-1a** and conducted the research using NMR and UV−vis (for details, see Part K−M in Supporting Information). It is known that the characteristic absorbance band of anionic **6HQNO′** of the N-oxide 6-hydroxyquinoline in methanol consisted of a peak at 385 nm, while that of the neutral **6HQNO** is 323 nm.[34] Due to that **QD-1a**/**QD-1a′** have very similar structural unit as in **6HQNO**/**6HQNO′**, **QD-1a** and **QD-1a′** could be expected to be differentiable by their absorbance spectra. And lucky enough, the coexistence of the zwitterion ion **QD-1a′** was indeed experimentally observed by UV−vis in the present work. Under neutral conditions, a strong absorbance with maxima at 327 nm, which is assigned to neutral **QD-1a**, is clearly observed (Figure 3, in green). A closer inspection further shows that there is also a notable weak absorbance from 370 to 440 nm (with the main peak at 395 nm), which was suspected to reflect the existence of the zwitterion ion **QD-1a′** in low concentration. This was later confirmed by varying the pH of the solution. Addition of an acid solution (HCl) into this system caused a total disappearance of the absorbance from 370 to 440 nm (Figure 3, in blue), while adding a basic solution (NaOH) resulted in a gradual increase of the band at 395 nm (Figure 3, in pink). These experimental results are clearly in line with the hypothesis from calculation.

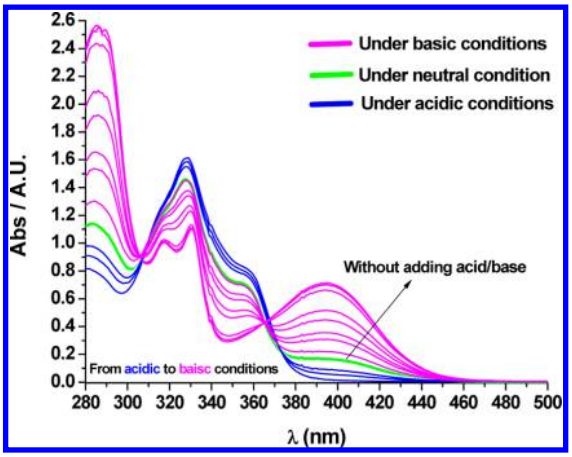

Figure 3. Variations of absorption spectra of **QD-1a** in methanol as added acid or base.

On the basis of the above, the third catalytic cycle in Scenario III could be envisaged. The **QD-1a** first converts to the zwitterion ion **QD-1a′**, in which the 6′-O^- unit functions as a base to deprotonate the α-proton of **R1**, while the protonated quinulcidine works as the hydrogen-bond donor to interact with the carbonyl oxygen of **R1**.

Figure 4 shows the calculated results. The binding of **R1** to **QD-1a′** is realized by hydrogen-bonding interaction between the protonated quinulcidine (N1−H10′) and the carbonyl oxygen (O1″) and forms **CP1e**, which is 8.2 kcal/mol above the separated reactant and catalyst. The hydrogen-bond distances, N1−H10′···O1″ and C6′−O9′···H7″ in **CP1e**, are 1.888 and 2.134 Å, respectively. Deprotonation of the α-proton (H7″) of **R1** by the 6′-O^- unit of **QD-1a′** proceeds via **TS1e** and has a barrier of 8.1 kcal/mol in free energy. The γ-protonation with 6′-OH as the proton donor proceeds via **TS2e(s)** and is the rate-limiting step in Scenario III, requiring an overall activation free energy of 18.1 kcal/mol.[36]

Reviewing the three mechanistic scenarios aforementioned, the γ-protonation was predicted to be the rate-limiting step in all these mechanistic pathways (Figure 5). This is in line with Deng's kinetic studies.[5] The overall activation free energy in Scenario III was predicted to be 1.7 and 8.0 kcal/mol lower than that in Scenarios I and II, respectively.

Thus, Scenario III should be the most favored mechanism for the **QD-1a** catalyzed isomerization of γ-methyl β,γ-butenolide to γ-methyl α,β-butenolide. Since Scenario III is only 1.7 kcal/mol favored over Scenario I, these two mechanisms could compete with one another. The more precise calculations using the M05-2x/6-311+G(2d,p)//M05-2x/6-31+G(d)(SMD) and B2PLYP-D/6-31+G(d,p)//M05-2x/6-31+G(d)(SMD) methods gave similar relative energies (see Figure S15).

The overall reaction was calculated to be exergonic by −1.0 kcal/mol. The formation of more stable conjugated α,β-unsaturated butenolides would be the driving force for these olefin isomerizations. Moreover, the calculation predicted that the isomerization of α,γ-dimethyl β,γ-butenolide (**R2**) to α,γ-dimethyl α,β-butenolide (**P2**) are exergonic by −4.9 kcal/mol (Scheme S2), explaining the intriguing experimental observation that the γ-methyl α,β-butenolide (**P1**) underwent easy racemization and that no detectable racemization was observed for the α,γ-disubstituted β,γ-unsaturated butenolides even at room temperature.

dx.doi.org/10.1021/ja309133z | J. Am. Chem. Soc. 2013, 135, 7462−7473

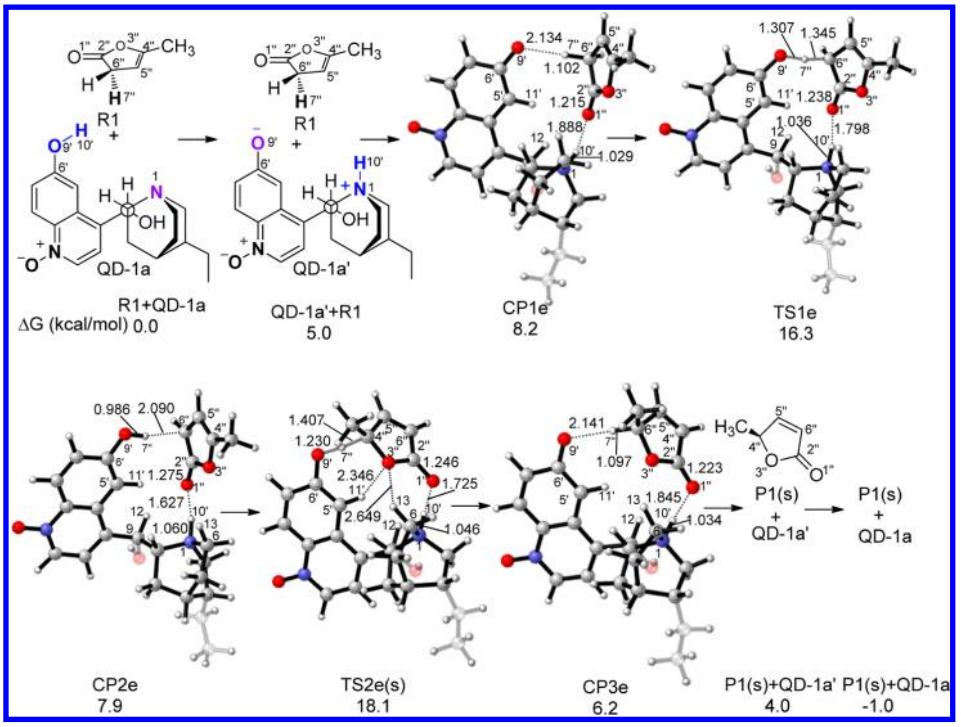

Figure 4. Energies and optimized geometries in Scenario III for the **QD-1a** catalyzed isomerization calculated with M05-2x/6-31+G(d)(SMD).

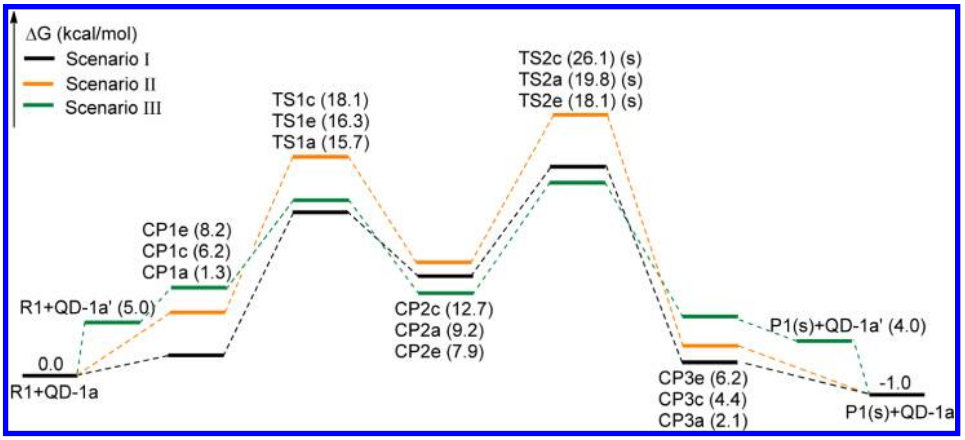

Figure 5. Potential energy surface of **QD-1a** catalyzed isomerization calculated with M05-2x/6-31+G(d)(SMD).

Origin of Selectivity of QD-1a Catalyzed Reaction. Since the γ-protonation is the rate-limiting and stereocontrolling step of the **QD-1a** catalyzed isomerization of **R1** to **P1** and the overall activation free barrier in Scenario II are at least 6 kcal/mol higher than that in Scenarios I or III, we focused our attention on the transition-state structures **TS2a(s)**, **TS2b(r)**, **TS2e(s)**, and **TS2f(r)** in discussing the origin of selectivity. According to the relative free energies (Figure 6), the major *s*-product observed in the **QD-1a** catalyzed isomerization should mainly arise from **TS2e(s)**, while the minor *r*-product from **TS2f(r)**. On the basis of the traditional transition state theory, the ee value of the **QD-1a** catalyzed isomerization of **R1** to **P1** can be evaluated by eq 1, where R is the ideal gas constant, T = 253.15. The predicated ee was 98%, which is very close to the experimental value 92%. Interestingly, the calculation using a model catalyst, in which the 9-OH was replaced by a hydrogen atom, gives 92% ee for the same isomerization (Figure S17). It suggests that 9-OH and the chirality at C9 have a minor effect on the selectivity.

$$\mathrm{ee} = \frac{\sum_i e^{-\Delta G^{\neq}_{\mathrm{rel}}(S_i)/RT} - \sum_i e^{-\Delta G^{\neq}_{\mathrm{rel}}(R_i)/RT}}{\sum_i e^{-\Delta G^{\neq}_{\mathrm{rel}}(S_i)/RT} + \sum_i e^{-\Delta G^{\neq}_{\mathrm{rel}}(R_i)/RT}} \quad (1)$$

Attractive noncovalent interactions in asymmetric catalysis have been considered as the links between enzymes and small molecule catalysts.[37] However, unraveling the weak interactions in transition states is nontrivial due to the subtle nature of these interactions. Recently, Yang and co-workers introduced an invaluable approach to identify noncovalent interactions on the basis of analyzing the electron densities and their reduced density gradient RDG isosurface.[19] Such analysis is known to be able to identify the location and strength of noncovalent interactions by examining the peaks that appear in the RDG at low densities. The analysis of the electron density and the RDG for the stereocontrolling transition-state structures of the **QD-1a** catalyzed isomerization of **R1** to **P1** was conducted by using the NCIPLOT[19] and Multiwfn.[38] The results are presented in Figure 6. It is clear that several stabilizing C−H···O[20,21] and C−

dx.doi.org/10.1021/ja309133z | J. Am. Chem. Soc. 2013, 135, 7462−7473

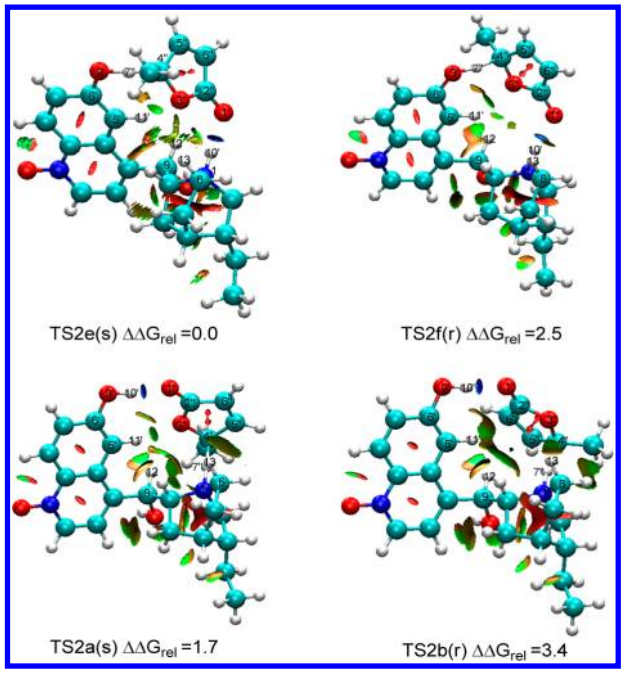

Figure 6. Noncovalent interaction analysis (blue, strong attraction; green, weak interaction; and red, strong repulsion) for stereocontrolling transition states in the **QD-1a** catalyzed isomerization, together with their relative free energies (kcal/mol), calculated with M05-2x/6-31+G(d)(SMD).

H···π interactions[39] are present in these transition-state structures. However, it is still not easy to discern which hydrogen bond is the major factor in governing selectivity. Therefore, quantitative description of the strength of the hydrogen bonds involved in the hydrogen-bond network in transition-state structures would be highly desirable, because it can be directly used to quantitatively interpret the origin of selectivity.

In recent years, there are numerous studies using quantum theory of atoms in molecules (QTAIM) to investigate the interatomic interactions in terms of the topological properties of electron density.[40] The analysis of the parameters derived from QTAIM, such as the electron density ($\rho_{(cp)}$) at the H···X (X = O, N) intermolecular bond critical point (BCP) and the laplacian of the electron density ($\nabla^2_{(cp)}$) at this BCP, was found to be very useful to deepen the understanding of the nature of hydrogen bond.[41] Espinosa and co-workers noted that the energy of a particular hydrogen bond (E_{int}) correlated with the local electron potential energy density $V(r_{cp})$ (eq 2).[42] With eq 2, one could give a quantitative description of the strength of hydrogen bonds in the hydrogen-bond network in transition-state structures.

$$E_{(int)} = \frac{1}{2}V(r_{cp}) \quad (2)$$

The estimated energies (E_{int}) of the hydrogen bonds involved in these stereocontrolling transition-state structures are summarized in Table 1. Notably, the hydrogen-bonding interaction between the H10′ and O1″ atoms in **TS2e(s)** is 1.9 kcal/mol stronger than that in **TS2f(r)** due to its shorter H10′···O1″ distance (1.725 in **TS2e(s)** vs 1.784 in **TS2f(r)**). Moreover, the favorable C9−H12···O1″ and C6−H13···O3″ interactions were found to contribute 1.5 and 1.4 kcal/mol to the stability of **TS2e(s)**, respectively. On the contrary, these two stabilizing interactions were absent in **TS2f(r)**. It should be pointed out that there is a comparable stabilizing C5′−H11′···O3″ interaction in both **TS2e(s)** (3.1 kcal/mol) and **TS2f(r)** (3.7 kcal/mol). Taking all these into account, the stabilizing C9−H12···O1″ and C6−H13···O3″ interactions and the stronger H10′···O1″ interaction cause **TS2e(s)** to behave differently from **TS2f(r)**, leading to the experimentally observed selectivity.

Though hydrogen-bonding interaction between the H10′ and O1″ atoms in **TS2a(s)** is only 0.4 kcal/mol weaker than that in **TS2b(r)**, the stabilizing interaction between H11′ and O3″ can contribute 3.3 kcal/mol to the stability of **TS2a(s)**, whereas no such stabilizing interaction is present in **TS2b(r)**. Moreover, the relatively weak C9−H12···O3″ and C5′−H11′···O1″ interactions (2.0 and 1.3 kcal/mol, respectively) in **TS2a(s)** as compared to those among H11′···π (C2″═C6″), H12···π (C5″═C6″), and C6−H13···O3″ (1.7, 1.3, and 1.4 kcal/mol, respectively) in **TS2b(r)** could also influence the stability of the former. Obviously, the presence of the medium strong C5′-H11′···O3″ interaction in **TS2a(s)** would be the main factor that makes it more stable than **TS2b(r)**.

In summary, though the conventional N−H···O or O−H···O hydrogen bonds give the most stable interactions in these transition-state structures, it is the multiple weak nonconventional C−H···O hydrogen bonds that induce selectivity of the **QD-1a** catalyzed olefin isomerization. The B2PLYP-D/6-31+G(d,p)// M05-2x/6-31+G(d)(SMD) method predicted very similar values for these weak nonconventional C−H···O hydrogen bonds (see Table S1).

From the stereocontrolling transition structure in Scenarios III and I, it seems that the methyl group at C4″ of substrate would not affect the selectivity through steric interaction. To provide further verification for the proposed mechanism, the effect of the substituent at C4″ of substrate was studied by using the *a*-isopropyl-*β*,*γ*-butenolide as a model substrate. The

Table 1. Estimated Strength of Hydrogen Bonds Involved in the Transition-State Structures for QD-1a and QD-1b Catalyzed Isomerization (kcal/mol)

TS	type of hydrogen bonds and its energy			
TS2a(s)	$E_{(H10'\cdots O1'')} = -11.7$	$E_{(H11'\cdots O3'')} = -3.3$	$E_{(H12\cdots O3'')} = -2.0$	$E_{(H11'\cdots O1'')} = -1.3$
TS2b(r)	$E_{(H10'\cdots O1'')} = -12.1$	$E_{(H11'\cdots \pi(C2''=C6''))} = -1.7$	$E_{(H12\cdots \pi(C5''=C6''))} = -1.3$	$E_{(H13\cdots O3'')} = -1.4$
TS2e(s)	$E_{(H10'\cdots O1'')} = -12.2$	$E_{(H11'\cdots O3'')} = -3.1$	$E_{(H12\cdots O1'')} = -1.5$	$E_{(H13\cdots O3'')} = -1.4$
TS2f(r)	$E_{(H10'\cdots O1'')} = -10.3$	$E_{(H11'\cdots O3'')} = -3.7$	–	–
2TS2a(s)	$E_{(H10'\cdots O1'')} = -11.6$	$E_{(H11'\cdots O3'')} = -3.3$	$E_{(H12\cdots O3'')} = -1.7$	–
2TS2b(r)	$E_{(H10'\cdots O1'')} = -11.5$	$E_{(H11'\cdots \pi(C2''=C6''))} = -1.7$	$E_{(H12\cdots \pi(C5''=C6''))} = -1.3$	$E_{(H13\cdots O3'')} = -1.3$
2TS2e(s)	$E_{(H10'\cdots O1'')} = -12.2$	$E_{(H11'\cdots O3'')} = -2.7$	$E_{(H12\cdots O1'')} = -1.8$	$E_{(H13\cdots O3'')} = -0.9$
2TS2f(r)	$E_{(H10'\cdots O1'')} = -11.3$	$E_{(H11'\cdots O3'')} = -2.2$	$E_{(H12\cdots O1'')} = -1.4$	–

dx.doi.org/10.1021/ja309133z | J. Am. Chem. Soc. 2013, 135, 7462−7473

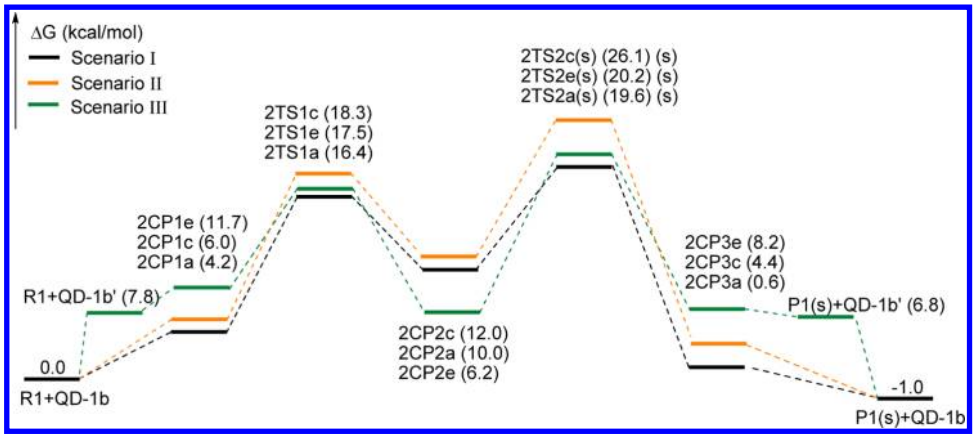

Figure 7. Potential energy surface of **QD-1b** catalyzed isomerization calculated with M05-2x/6-31+G(d)(SMD).

calculated ee values for the **QD-1a** catalyzed isomerization of methyl and isopropyl substituted-β,γ-butenolide are nearly identical (see Figure S18), which is in accord with Deng and co-workers' experimental observation.

Mechanism of QD-1b Catalyzed Reaction. In the early stage of asymmetric catalysis, considerable efforts were devoted to the role of steric repulsion in designing chiral catalysts.[43] Recently, manipulation of electronic effect of catalyst gained increasing attention.[6] Deng and co-workers' work was just one of the successful applications of the "electronic tuning of the catalyst" strategy. By rational oxidization of the quinoline ring N of **QD-1b** into its N-oxide analogue **QD-1a**, they achieved a significant enhancement of the catalytic activity and selectivity.[5] So, it is of great interest to compare the structures and energies of the intermediates and transition states involved in the **QD-1b** and **QD-1a** catalyzed isomerizations. The information deduced from the electronic effect of catalyst on activity and selectivity would be very helpful for the design of new catalysts.

The optimized transition-state and intermediate structures in the **QD-1b** catalyzed isomerization resemble those in the **QD-1a** catalyzed pathway (see Figures S19–S24). Similarly, the γ-protonation step is showed to be rate limiting for **QD-1b** catalyzed isomerization of **R1** to **P1** (Figure 7). However, the different acidity of the 6′-OH group in **QD-1b** and **QD-1a** makes differences! Contrasting to the **QD-1a** catalyzed isomerization, the calculated overall activation free energy in Scenario I is 0.6 kcal/mol lower than that in Scenario III for the **QD-1b** catalyzed isomerization. This suggests that the protonated quinuclidine become a better proton donor than the 6′-OH for the catalyst **QD-1b** due to the decreased acidity of its 6′-OH group. In other words, **QD-1b** is slightly more preferred to utilize protonated quinuclidine, whereas **QD-1a** is more preferred to 6′-OH as proton donor in the stereo-controlling step. Thus, the present calculations reveal that the catalytic mode of a given catalytic reaction may change when tuning the catalyst by varying its electronic effect.

Moreover, when the 6′-OH group functions as proton donor in the stereocontrolling step, the overall activation free energy of the **QD-1a** catalyzed reaction is 2.1 kcal/mol lower than that of the **QD-1b** catalyzed isomerization (Scenario III in Figures 5 and 7). On the other hand, when the 6′-OH group acts a hydrogen donor in the stereocontrolling step, the overall activation free energies of the **QD-1a** and **QD-1b** catalyzed isomerization are almost the same (Scenario I in Figures 5 and 7). Thus, one can reach the conclusion that enhancing the acidity of the 6′-OH group has an obvious effect on catalytic activity when it acts as a proton donor.

In addition, the **QD-1b** catalyzed isomerization via Scenario I requires 19.6 kcal/mol activation free energy, which is 1.5 kcal/mol greater than that of the **QD-1a** catalyzed same isomerization via Scenario III (calculations using the M05-2x/6-311+G(2d,p)//M05-2x/6-31+G(d)(SMD) and B2PLYP-D/6-31+G(d,p)//M05-2x/6-31+G(d)(SMD) methods predicted similar relative energies; see Figure S16). This explains the observed lower catalytic activity of **QD-1b**.

Origin of Decreased Selectivity of QD-1b Catalyzed Reaction. Catalyst **QD-1b** has not only a lower catalytic activity but also a lower selectivity than those of **QD-1a**[5] that correspond well with our calculation. The free energy difference was found by calculation to be only 0.9 kcal/mol between **2TS2a(s)** and **2TS2b(r)** and 0.4 kcal/mol between **2TS2e(s)** and **2TS2f(r)** (Figure 8), resulting in a predicted ee of 62%.

Through inspection of the structure of **2TS2a(s)** and **TS2a(s)**, it is clear that the H10′···O1″ distance in **2TS2a(s)** is longer than that in **TS2a(s)** (1.712 Å vs 1.707 Å). This suggests that **R1** should bind looser with **QD-1b** than with **QD-1a** due to the low acidity of the 6′-OH group in the former. Consequently, some hydrogen-bonding interactions become weakened or even vanished in **2TS2a(s)** (Table 1). For example, the favorable C9–H12···O3″ interaction, which contributed 2.0 kcal/mol to the stability of **TS2a(s)**, becomes weakened to 1.7 kcal/mol in **2TS2a(s)** as a result of H12···O3″ distance lengthening from 2.522 to 2.577 Å; and the C5′-H11′···O1″ interaction, which contributed 1.3 kcal/mol to stabilizing **TS2a(s)**, now shows a negligible effect on stability of **2TS2a(s)** due to extension of the H11′···O1″ distance. On the other hand, the stabilizing C5′–H11′···O3″ interaction remained unchanged due to similar bonding length in **TS2a(s)** and in **2TS2a(s)**. Besides, though the O9′–H10′···O1″ interaction is weakened from 12.1 kcal/mol in **TS2b(r)** to 11.5 kcal/mol in **2TS2b(r)**, the favorable C6–H13···O3′, H11′···π (C2″=C6″), and H12···π (C5″=C6″) interactions were about the same in **TS2b(r)** and **2TS2b(r)**. That is, the **2TS2a(s)** favored over **2TS2b(r)** altogether by only 0.9 kcal/mol. Similarly, the stabilizing C5′–H11′···O3″ and C6–H13···O3″ interactions in **2TS2e(s)** reduced to 2.7 and 0.88 kcal/mol as their distance increased to 2.411 and 2.822 Å, respectively. The stabilizing C5′–H11′···O3″ interaction reduced from 3.7 kcal/mol in **TS2f(r)** to 2.2 kcal/mol in **2TS2f(r)** as the H11′···O3″ distance lengthened from 2.268 to 2.488 Å.

dx.doi.org/10.1021/ja309133z | J. Am. Chem. Soc. 2013, 135, 7462–7473

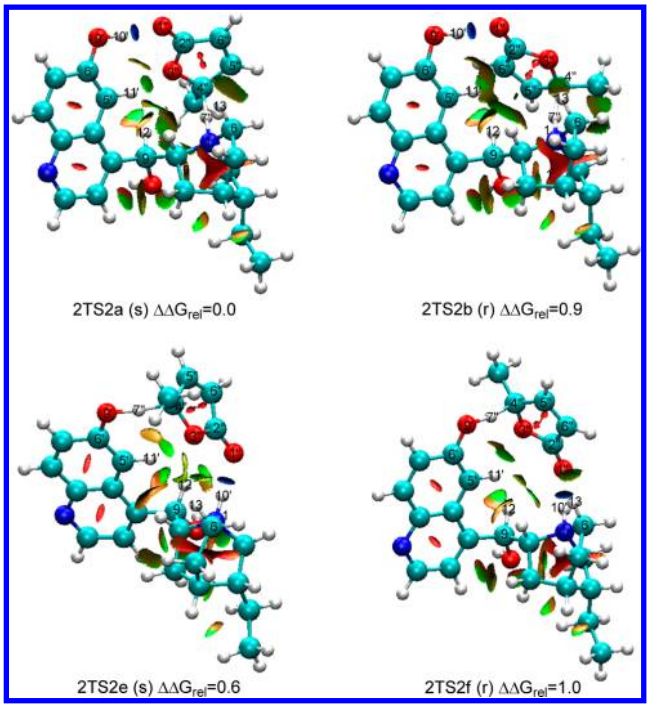

Figure 8. Noncovalent interaction analysis (blue, strong attraction; green, weak interaction; and red, strong repulsion) for stereocontrolling transition states in the **QD-1b** catalyzed isomerization, together with their relative free energies (kcal/mol), calculated with M05-2x/6-31+G(d) (SMD).

Overall, the computationally predicted decrease of enantioselectivity in the **QD-1b** catalyzed isomerization of γ-methyl β,γ-butenolide to γ-methyl α,β-butenolide is in good agreement with experiment. The reduced enantioselectivity is originated from the looser hydrogen binding of substrate **R1** with catalyst **QD-1b** than with **QD-1a**, and this causes an attenuation of the stabilizing nonconventional hydrogen interactions in the stereocontrolling transition-state structures of the **QD-1b** catalyzed reaction.

4. CONCLUSION

Computational study of the asymmetric olefin isomerization of β,γ- to α,β-unsaturated butenolides catalyzed by cinchona alkaloid derivatives yielded important mechanistic insights into the bioinspired proton-transfer catalysis. First, the computation showed that the γ-protonation step is rate limiting in olefin isomerization and that both the protonated quinuclidine and 6′-OH of the catalyst may function as proton donor in the stereocontrolling step. Second, it was found that **QD-1a** prefers to utilize 6′-OH, whereas **QD-1b** prefers slightly more to protonated quinuclidine as proton donor in the stereocontrolling step. Thus, a catalytic reaction may proceed via different pathways when the catalyst is modified simply by tuning its electronic effect. Third, the noncovalent interactions in the stereocontrolling transition state were identified, and their strengths were estimated quantitatively. The selectivity of the cinchona alkaloids catalyzed asymmetric olefin isomerization of β,γ- to α,β-unsaturated butenolides arises mainly from the multiple nonconventional C−H···O hydrogen-bonding interactions. The experimentally observed lower stereoselectivity for this catalytic olefin isomerization with **QD-1b** than with **QD-1a** was reproduced by computation and was rationalized by the looser hydrogen binding of **QD-1b** with substrate as compared to the case of **QD-1a**, which was verified to be the primary factor leading to a reduction of the nonconventional hydrogen-bonding interactions in the stereocontrolling transition state. In sum, the present calculation suggested that, for certain acid−base bifunctional chiral catalysts, the acid−base active sites of catalysts may interconvert and yield new catalyst varieties with higher activity and selectivity. This study is thus believed to contribute to a better understanding of the so-called "electronic tuning of asymmetric catalyst",[6d] and to provide useful hints for designing the cinchona alkaloids and other acid−base bifunctional chiral catalysts promoted reactions.

■ ASSOCIATED CONTENT

Supporting Information

Figures S1−S31, Schemes S1−S4, a complete citation for ref 26, experimental details, and optimized geometries and energies of all computed species. This material is available free of charge via the Internet at http://pubs.acs.org.

■ AUTHOR INFORMATION

Corresponding Author

esr@nankai.edu.cn; chengjp@most.cn

Notes

The authors declare no competing financial interest.

■ ACKNOWLEDGMENTS

The authors are highly appreciative of the financial support from the National Natural Science Foundation of China (NSFC grant nos. 21172112, 51173083, and 21172118) and the National Basic Research Program of China (2010CB833300 and 2012CB821600). The reviewers' very valuable comments and especially the suggestion of one reviewer to find experimental evidence for the computationally proposed role of **QD-1a′** are greatly acknowledged.

■ REFERENCES

(1) (a) Xue, L.; Talalay, P.; Mildvan, A. S. *Biochemistry* **1990**, *29*, 7491. (b) Austin, J. C.; Kuliopulos, A.; Mildvan, A. S.; Spiro, T. G. *Protein Sci.* **1992**, *1*, 259. (c) Hawkinson, D. C.; Pollack, R. M.; Ambulos, N. P. *Biochemistry* **1994**, *33*, 12172. (d) Zhao, Q.; Abeygunawardana, C.; Talalay, P.; Mildvan, A. S. *Proc. Natl. Acad. Sci. U.S.A.* **1996**, *93*, 8220. (e) Zhao, Q. J.; Abeygunawardana, C.; Gittis, A. G.; Mildvan, A. S. *Biochemistry* **1997**, *36*, 14616. (f) Massiah, M. A.; Abeygunawardana, C.; Gittis, A. G.; Mildvan, A. S. *Biochemistry* **1998**, *37*, 14701.

(2) For selected reviews, see: (a) Breslow, R. *Acc. Chem. Res.* **1995**, *28*, 146. (b) Kirby, A. J. *Angew. Chem., Int. Ed.* **1996**, *35*, 706. (c) Marchetti, L.; Levine, M. *ACS Catal.* **2011**, *1*, 1090. (d) Bernardi, L.; Fochi, M.; Franchini, M. C.; Ricci, A. *Org. Biomol. Chem.* **2012**, *10*, 2911.

(3) For selected reviews, see: (a) *Acc. Chem. Res.* **2004**, *37*(8), special issue on organocatalysis. (b) Berkessel, A.; Groger, H. *Asymmetric Organocatalysis*; Wiley-VCH: Weinheim, Germany, 2005. (c) *Chem. Rev.* **2007**, *107*(12), special issue on organocatalysis. (d) Dalko, P. I. *Enantioselective Organocatalysis*; Wiley-VCH: Weinheim, 2007. (e) *Proc. Natl. Acad. Sci. U.S.A.* **2010**, *107*(48), special feature issue on organocatalysis.

(4) (a) Hintermann, L.; Schmitz, M. *Adv. Synth. Catal.* **2008**, *350*, 1469. (b) Saga, Y.; Motoki, R.; Makino, S.; Shimizu, Y.; Kanai, M.; Shibasaki, M. *J. Am. Chem. Soc.* **2010**, *132*, 7905. (c) Wu, Y.; Deng, L. *J. Am. Chem. Soc.* **2012**, *134*, 14334. (d) Lee, J. H.; Deng, L. *J. Am. Chem. Soc.* **2012**, *134*, 18209.

(5) Wu, Y.; Singh, R. P.; Deng, L. *J. Am. Chem. Soc.* **2011**, *133*, 12458.

(6) For recent reviews, see: (a) Flanagan, S. P.; Guiry, P. J. *J. Organomet. Chem.* **2006**, *691*, 2125. (b) Xu, J. X. *Curr. Org. Synth.* **2010**, *7*, 650. For select examples (c) Hughes, D. L.; Dolling, U. H.; Ryan, K. M.; Schoenewaldt, E. F.; Grabowski, E. J. J. *J. Org. Chem.* **1987**, *52*, 4745. (d) Jacobsen, E. N.; Zhang, W.; Guler, M. L. *J. Am. Chem. Soc.* **1991**, *113*, 6703. (e) RajanBabu, T. V.; Casalnuovo, A. L. *J. Am. Chem. Soc.* **1992**, *114*, 6265. (f) Nelson, D. W.; Gypser, A.; Ho, P. T.; Kolb, H. C.; Kondo, T.; Kwong, H. L.; McGrath, D. V.; Rubin, A. E.; Norrby, P. O.; Gable, K. P.; Sharpless, K. B. *J. Am. Chem. Soc.* **1997**, *119*, 1840. (g) Palucki, M.; Finney, N. S.; Pospisil, P. J.; Guler, M. L.; Ishida, T.; Jacobsen, E. N. *J. Am. Chem. Soc.* **1998**, *120*, 948. (h) Yang, D.; Yip, Y.-C.; Chen, J.; Cheung, K.-K. *J. Am. Chem. Soc.* **1998**, *120*, 7659. (i) RajanBabu, T. V.; Radetich, B.; You, K. K.; Ayers, T. A.; Casalnuovo, A. L.; Calabrese, J. C. *J. Org. Chem.* **1999**, *64*, 3429. (j) Tang, Z.; Jiang, F.; Cui, X.; Gong, L. Z.; Mi, A. Q.; Jiang, Y. Z.; Wu, Y. D. *Proc. Natl. Acad. Sci. U.S.A.* **2004**, *101*, 5755. (k) Xu, J. X.; Wei, T. Z.; Zhang, Q. H. *J. Org. Chem.* **2004**, *69*, 6860. (l) Jeulin, S.; de Paule, S. D.; Ratovelomanana-Vidal, V.; Genet, J. P.; Champion, N.; Dellis, P. *Proc. Natl. Acad. Sci. U.S.A.* **2004**, *101*, 5799. (m) Yan, X. X.; Peng, Q.; Zhang, Y.; Zhang, K.; Hong, W.; Hou, X. L.; Wu, Y. D. *Angew. Chem., Int. Ed.* **2006**, *45*, 1979. (n) Jensen, K. H.; Sigman, M. S. *Angew. Chem., Int. Ed.* **2007**, *46*, 4748. (o) Ganesh, M.; Seidel, D. *J. Am. Chem. Soc.* **2008**, *130*, 16464. (p) Yan, X.-X.; Peng, Q.; Li, Q.; Zhang, K.; Yao, J.; Hou, X.-L.; Wu, Y.-D. *J. Am. Chem. Soc.* **2008**, *130*, 14362. (q) Wu, H.-C.; Hamid, A. A.; Yu, J.-Q.; Spencer, J. B. *J. Am. Chem. Soc.* **2009**, *131*, 9604. (r) Korenaga, T.; Nomura, K.; Onoue, K.; Sakai, T. *Chem. Commun.* **2010**, *46*, 8624. (s) Jensen, K. H.; Sigman, M. S. *J. Org. Chem.* **2010**, *75*, 7194. (t) Harper, K. C.; Sigman, M. S. *Science* **2011**, *333*, 1875. (u) So, S. S.; Burkett, J. A.; Mattson, A. E. *Org. Lett.* **2011**, *13*, 716. (v) So, S. S.; Mattson, A. E. *J. Am. Chem. Soc.* **2012**, *134*, 8798. (w) Vermoortele, F.; Vandichel, M.; Van de Voorde, B.; Ameloot, R.; Waroquier, M.; Van Speybroeck, V.; De Vos, D. E. *Angew. Chem., Int. Ed.* **2012**, *51*, 4887. (x) Xu, X.; Liu, P.; Lesser, A.; Sirois, L. E.; Wender, P. A.; Houk, K. N. *J. Am. Chem. Soc.* **2012**, *134*, 11012.

(7) Alali, F. Q.; Liu, X.-X.; McLaughlin, J. L. *J. Nat. Prod.* **1999**, *62*, 504.

(8) For selected examples, see: (a) de March, P.; Figueredo, M.; Font, J.; Raya, J.; Alvarez-Larena, A.; Piniella, J. F. *J. Org. Chem.* **2003**, *68*, 2437. (b) Yoshimitsu, T.; Makino, T.; Nagaoka, H. *J. Org. Chem.* **2004**, *69*, 1993. (c) Gao, S.; Wang, Q.; Chen, C. *J. Am. Chem. Soc.* **2009**, *131*, 1410.

(9) For selected recent examples, see: (a) Brown, S. P.; Goodwin, N. C.; MacMillan, D. W. C. *J. Am. Chem. Soc.* **2003**, *125*, 1192. (b) Braukmüller, S.; Brüuckner, R. *Eur. J. Org. Chem.* **2006**, 2110. (c) Kapferer, T.; Brückner, R. *Eur. J. Org. Chem.* **2006**, 2119. (d) Geurts, K.; Fletcher, S. P.; Feringa, B. L. *J. Am. Chem. Soc.* **2006**, *128*, 15572. (e) Yamaguchi, A.; Matsunaga, S.; Shibasaki, M. *Org. Lett.* **2008**, *10*, 2319. (f) Trost, B. M.; Hitce, J. *J. Am. Chem. Soc.* **2009**, *131*, 4572. (g) Zhang, Y.; Yu, C.; Ji, Y.; Wang, W. *Chem.—Asian J.* **2010**, *5*, 1303. (h) Wang, J.; Qi, C.; Ge, Z.; Cheng, T.; Li, R. *Chem. Commun.* **2010**, *46*, 2124. (i) Ube, H.; Shimada, N.; Terada, M. *Angew. Chem., Int. Ed.* **2010**, *49*, 1858. (j) Cui, H.; Huang, J.; Lei, J.; Wang, Z.; Chen, S.; Wu, L.; Chen, Y. *Org. Lett.* **2010**, *12*, 720. (k) Yang, Y.; Zheng, K.; Zhao, J. N.; Shi, J. A.; Lin, L. L.; Liu, X. H.; Feng, X. M. *J. Org. Chem.* **2010**, *75*, 5382. (l) Zhou, L.; Lin, L. L.; Ji, J.; Xie, M. S.; Liu, X. H.; Feng, X. M. *Org. Lett.* **2011**, *13*, 3056. (m) Pansare, S. V.; Paul, E. K. *Chem. Commun.* **2011**, *47*, 1027. (n) Mao, B.; Geurts, K.; Fañanás-Mastral, M.; van Zijl, A. W.; Fletcher, S. P.; Minnaard, A. J.; Feringa, B. L. *Org. Lett.* **2011**, *13*, 948.

(10) For representative examples, see: (a) Bahmanyar, S.; Houk, K. N. *J. Am. Chem. Soc.* **2001**, *123*, 11273. (b) Bahmanyar, S.; Houk, K. N. *J. Am. Chem. Soc.* **2001**, *123*, 12911. (c) Rankin, K. N.; Gauld, J. W.; Boyd, R. J. *J. Phys. Chem. A* **2002**, *106*, 5155. (d) Clemente, F. R.; Houk, K. N. *Angew. Chem., Int. Ed.* **2004**, *43*, 5766. For reviews: (e) Allemann, C.; Gordillo, R.; Clemente, F. R.; Cheong, P. H. Y.; Houk, K. N. *Acc. Chem. Res.* **2004**, *37*, 558. (f) Sunoj, R. B. *WIREs Comput. Mol. Sci.* **2011**, *1*, 920 and references cited therein..

(11) For selected examples, see: (a) Schreiner, P. R.; Wittkopp, A. *Org. Lett.* **2002**, *4*, 217. (b) Dudding, T.; Houk, K. N. *Proc. Natl. Acad. Sci. U.S.A.* **2004**, *101*, 5770. (c) Xu, S. J.; Held, I.; Kempf, B.; Mayr, H.; Steglich, W.; Zipse, H. *Chem.—Eur. J.* **2005**, *11*, 4751. (d) Singleton, D. A.; Wang, Z. H. *J. Am. Chem. Soc.* **2005**, *127*, 6679. (e) Gordillo, R.; Houk, K. N. *J. Am. Chem. Soc.* **2006**, *128*, 3543. (f) Zhang, X.; Du, H.; Wang, Z.; Wu, Y.-D.; Ding, K. *J. Org. Chem.* **2006**, *71*, 2862. (g) Hamza, A.; Schubert, G.; Soós, T.; Pápai, I. *J. Am. Chem. Soc.* **2006**, *128*, 13151. (h) Yamanaka, M.; Itoh, J.; Fuchibe, K.; Akiyama, T. *J. Am. Chem. Soc.* **2007**, *129*, 6756. (i) Xia, Y.; Liang, Y.; Chen, Y.; Wang, M.; Jiao, L.; Huang, F.; Liu, S.; Li, Y.; Yu, Z.-X. *J. Am. Chem. Soc.* **2007**, *129*, 3470. (j) Kirsten, M.; Rehbein, J.; Hiersemann, M.; Strassner, T. *J. Org. Chem.* **2007**, *72*, 4001. (k) Fu, A. P.; Li, H. L.; Yuan, S. P.; Si, H. G.; Duan, Y. B. *J. Org. Chem.* **2008**, *73*, 5264. (l) Li, X.; Ye, S.; He, C.; Yu, Z.-Y. *Eur. J. Org. Chem.* **2008**, *25*, 4296. (m) Zuend, S. J.; Jacobsen, E. N. *J. Am. Chem. Soc.* **2009**, *131*, 15358. (n) Um, J. M.; Gutierrez, O.; Schoenebeck, F.; Houk, K. N.; MacMillan, D. W. C. *J. Am. Chem. Soc.* **2010**, *132*, 6001. (o) Uyeda, C.; Jacobsen, E. N. *J. Am. Chem. Soc.* **2011**, *133*, 5062. (p) Lu, T. X.; Zhu, R. X.; An, Y.; Wheeler, S. E. *J. Am. Chem. Soc.* **2012**, *134*, 3095. (q) Lam, Y. -h.; Houk, K. N.; Scheffler, U.; Mahrwald, R. *J. Am. Chem. Soc.* **2012**, *134*, 6286.

(12) (a) Houk, K. N.; Cheong, P. H. Y. *Nature* **2008**, *455*, 309. (b) Cheong, P. H. Y.; Legault, C. Y.; Um, J. M.; Celebi-Ölcüm, N.; Houk, K. N. *Chem. Rev.* **2011**, *111*, 5042.

(13) For preliminary reports: (a) Helder, R.; Arends, R.; Bolt, W.; Hiemstra, H.; Wynberg, H. *Tetrahedron. Lett.* **1977**, 2181. (b) Hiemstra, H.; Wynberg, H. *J. Am. Chem. Soc.* **1981**, *103*, 417. For recent reviews, see: (c) Kacprzak, K.; Gawronski, J. *Synthesis* **2001**, 961. (d) Tian, S. K.; Chen, Y. G.; Hang, J. F.; Tang, L.; McDaid, P.; Deng, L. *Acc. Chem. Res.* **2004**, *37*, 621. (e) Chen, Y. C. *Synlett.* **2008**, *13*, 1919. (f) Bartoli, G.; Melchiorre, P. *Synlett.* **2008**, *12*, 1759. (g) Song, C. E. *Cinchona Alkaloids in Synthesis and Catalysis: Ligands, Immobilization and Organocatalysis*, Song, C. E., Ed, Wiley-VCH, Weinheim, Germany, 2009. (h) Marcelli, T.; Hiemstra, H. *Synthesis* **2010**, 1229. (i) Jiang, L.; Chen, Y. C. *Catal. Sci. Technol.* **2011**, *1*, 354. (j) Yeboah, E. M. O.; Yeboah, S. O.; Singh, G. S. *Tetrahedron.* **2011**, *67*, 1725. (k) Melchiorre, P. *Angew. Chem., Int. Ed.* **2012**, *51*, 2.

(14) For examples of 6′-OH cinchona alkaloids, see: (a) Iwabuchi, Y.; Nakatani, M.; Yokoyama, N.; Hatakeyama, S. *J. Am. Chem. Soc.* **1999**, *121*, 10219. (b) Li, H. M.; Wang, Y.; Tang, L.; Deng, L. *J. Am. Chem. Soc.* **2004**, *126*, 9906. (c) Li, H. M.; Song, J.; Liu, X. F.; Deng, L. *J. Am. Chem. Soc.* **2005**, *127*, 8948. (d) Li, H. M.; Wang, Y.; Tang, L.; Wu, F. H.; Liu, X. F.; Guo, C. Y.; Foxman, B. M.; Deng, L. *Angew. Chem.,Int. Ed.* **2005**, *44*, 105. (e) Li, H. M.; Wang, B. M.; Deng, L. *J. Am. Chem. Soc.* **2006**, *128*, 732. (f) Wu, F. H.; Hong, R.; Khan, J. H.; Liu, X. F.; Deng, L. *Angew. Chem., Int. Ed.* **2006**, *45*, 4301. (g) Wang, Y.; Liu, X. F.; Deng, L. *J. Am. Chem. Soc.* **2006**, *128*, 3928. (h) Wang, B. M.; Wu, F. H.; Wang, Y.; Liu, X. F.; Deng, L. *J. Am. Chem. Soc.* **2007**, *129*, 768. (i) Wang, Y.; Li, H. M.; Wang, Y. Q.; Liu, Y.; Foxman, B. M.; Deng, L. *J. Am. Chem. Soc.* **2007**, *129*, 6364. (j) van Steenis, D. J. V. C.; Marcelli, T.; Lutz, M.; Spek, A. L.; van Maarseveen, J. H.; Hiemstra, H. *Adv. Synth. Catal.* **2007**, *349*, 281. (k) Liu, Y.; Provencher, B. A.; Bartelson, K. J.; Deng, L. *Chem. Sci.* **2011**, *2*, 1301. (l) Bartelson, K. J.; Singh, R. P.; Foxman, B. M.; Deng, L. *Chem. Sci.* **2011**, *2*, 1940. (m) Xiao, X.; Xie, Y.; Su, C.; Liu, M.; Shi, Y. *J. Am. Chem. Soc.* **2011**, *133*, 12914.

(15) For examples of C-9 substituted (thio)urea-, sulfonamide-, and squaramide derivatives, see: (a) Li, B. J.; Jiang, L.; Liu, M.; Chen, Y. C.; Ding, L. S.; Wu, Y. *Synlett* **2005**, 603. (b) Vakulya, B.; Varga, S.; Csámpai, A.; Soós, T. *Org. Lett.* **2005**, *7*, 1967. (c) McCooey, S. H.; Connon, S. J. *Angew. Chem., Int. Ed.* **2005**, *44*, 6367. (d) Song, J.; Wang, Y.; Deng, L. *J. Am. Chem. Soc.* **2006**, *128*, 6048. (e) Wang, Y. Q.; Song, J.; Hong, R.; Li, H. M.; Deng, L. *J. Am. Chem. Soc.* **2006**, *128*, 8156. (f) Connon, S. J. *Chem.;Eur. J.* **2006**, *12*, 5418. (g) Marcelli, T.; van der Haas, R. N. S.; van Maarseveen, J. H.; Hiemstra, H. *Angew. Chem., Int. Ed.* **2006**, *45*, 929. (h) Wang, J.; Li, H.; Zu, L.; Jiang, W.; Xie, H.; Duan, W.; Wang, W. *J. Am. Chem. Soc.* **2006**, *128*, 12652. (i) Diner, P.; Nielsen, M.; Bertelsen, S.; Niess, B.; Jorgensen, K. A. *Chem. Commun.* **2007**, 3646. (j) Oh, S. H.; Rho, H. S.; Lee, J. W.; Lee, J. E.; Youk, S. H.; Chin, J.; Song, C. E. *Angew. Chem., Int. Ed.* **2008**, *47*,

7872. (k) Malerich, J. P.; Hagihara, K.; Rawal, V. H. *J. Am. Chem. Soc.* **2008**, *130*, 14416. (l) Connon, S. J. *Synlett* **2009**, 354. (m) Liu, Y.; Sun, B. F.; Wang, B. M.; Wakem, M.; Deng, L. *J. Am. Chem. Soc.* **2009**, *131*, 418. (n) Lee, J. W.; Ryu, T. H.; Oh, J. S.; Bae, H. Y.; Bin Jang, H.; Song, C. E. *Chem. Commun.* **2009**, 7224. (o) Konishi, H.; Lam, T. Y.; Malerich, J. P.; Rawal, V. H. *Org. Lett.* **2010**, *12*, 2028. (p) Zhu, Y.; Malerich, J. P.; Rawal, V. H. *Angew. Chem., Int. Ed.* **2010**, *49*, 153. (q) Park, S. E.; Nam, E. H.; Bin Jang, H.; Oh, J. S.; Some, S.; Lee, Y. S.; Song, C. E. *Adv. Synth. Catal.* **2010**, *352*, 2211. (r) Peschiulli, A.; Procuranti, B.; O' Connor, C. J.; Connon, S. J. *Nat. Chem.* **2010**, *2*, 380. (s) Gleeson, O.; Davies, G.-L.; Peschiulli, A.; Tekoriute, R.; Gun'ko, Y. K.; Connon, S. J. *Org. Biomol. Chem.* **2011**, *9*, 7929. (t) Asano, K.; Matsubara, S. *J. Am. Chem. Soc.* **2011**, *133*, 16711. (u) Cornaggia, C.; Manoni, F.; Torrente, E.; Tallon, S.; Connon, S. J. *Org. Lett.* **2012**, *14*, 1850. (v) Curti, C.; Rassu, G.; Zambrano, V.; Pinna, L.; Pelosi, G.; Sartori, A.; Battistini, L.; Zanardi, F.; Casiraghi, G. *Angew. Chem., Int. Ed.* **2012**, *51*, 6200. (w) Albertshofer, K.; Tan, B.; Barbas, C. F., III *Org. Lett.* **2012**, *14*, 1834.

(16) For examples of cinchona alkaloid primary amine derivatives, see: (a) Chen, W.; Du, W.; Duan, Y.-Z.; Wu, Y.; Yang, S.-Y.; Chen, Y.-C. *Angew. Chem., Int. Ed.* **2007**, *46*, 7667. (b) Xie, J.-W.; Yue, L.; Chen, W.; Du, W.; Zhu, J.; Deng, J.-G.; Chen, Y.-C. *Org. Lett.* **2007**, *9*, 413. (c) Bartoli, G.; Bosco, M.; Carlone, A.; Pesciaioli, F.; Sambri, L.; Melchiorre, P. *Org. Lett.* **2007**, *9*, 1403. (d) Xie, J.-W.; Chen, W.; Li, R.; Zeng, M.; Du, W.; Yue, L.; Chen, Y.-C.; Wu, Y.; Zhu, J.; Deng, J.-G. *Angew. Chem., Int. Ed.* **2007**, *46*, 389. (e) McCooey, S. H.; Connon, S. J. *Org. Lett.* **2007**, *9*, 599. (f) Zhou, J.; Wakchaure, V.; Kraft, P.; List, B. *Angew. Chem., Int. Ed.* **2008**, *47*, 7656. (g) Singh, R. P.; Bartelson, K.; Wang, Y.; Su, H.; Lu, X.; Deng, L. *J. Am. Chem. Soc.* **2008**, *130*, 2422. (h) Lu, X. J.; Deng, L. *Angew. Chem., Int. Ed.* **2008**, *47*, 7710. (i) Gogoi, S.; Zhao, C.-G.; Ding, D. *Org. Lett.* **2009**, *11*, 2249. (j) Lu, X. J.; Liu, Y.; Sun, B. F.; Cindric, B.; Deng, L. *J. Am. Chem. Soc.* **2008**, *130*, 8134. (k) Wu, L.-Y.; Bencivenni, G.; Mancinelli, M.; Mazzanti, A.; Bartoli, G.; Melchiorre, P. *Angew. Chem., Int. Ed.* **2009**, *48*, 7196. (l) Bencivenni, G.; Wu, L.-Y.; Mazzanti, A.; Giannichi, B.; Pesciaioli, F.; Song, M.-P.; Bartoli, G.; Melchiorre, P. *Angew. Chem., Int. Ed.* **2009**, *48*, 7200. (m) Paixao, M. W.; Holub, N.; Vila, C.; Nielsen, M.; Jorgensen, K. A. *Angew. Chem., Int. Ed.* **2009**, *48*, 7338. (n) Zhang, E.; Fan, C.-A.; Tu, Y.-Q.; Zhang, F.-M.; Song, Y.-L. *J. Am. Chem. Soc.* **2009**, *131*, 14626. (o) Lifchits, O.; Reisinger, C. M.; List, B. *J. Am. Chem. Soc.* **2010**, *132*, 10227. (p) Bencivenni, G.; Galzerano, P.; Mazzanti, A.; Bartoli, G.; Melchiorre, P. *Proc. Natl. Acad. Sci. U.S.A.* **2010**, *107*, 20642. (q) Holub, N.; Jiang, H.; Paixao, M. W.; Tiberi, C.; Jorgensen, K. A. *Chem.—Eur. J.* **2010**, *16*, 4337. (r) Qiao, Z.; Shafiq, Z.; Liu, L.; Yu, Z.-B.; Zheng, Q.-Y.; Wang, D.; Chen, Y.-J. *Angew. Chem., Int. Ed.* **2010**, *49*, 7294. (s) Tan, B.; Candeias, N. R.; Barbas, C. F., III *Nat. Chem.* **2011**, *3*, 473. (t) Kwiatkowski, P.; Beeson, T. D.; Conrad, J. C.; MacMillan, D. W. C. *J. Am. Chem. Soc.* **2011**, *133*, 1738. (u) Tian, X.; Cassani, C.; Liu, Y.; Moran, A.; Urakawa, A.; Galzerano, P.; Arceo, E.; Melchiorre, P. *J. Am. Chem. Soc.* **2011**, *133*, 17934. (v) Cai, Q.; You, S.-L. *Org. Lett.* **2012**, *14*, 3040.

(17) (a) Vayner, G.; Houk, K. N.; Sun, Y. K. *J. Am. Chem. Soc.* **2004**, *126*, 199. (b) Hammar, P.; Marcelli, T.; Hiemstra, H.; Himo, F. *Adv. Synth. Catal.* **2007**, *349*, 2537. (c) Celebi-Ölcüm, N.; Aviyente, V.; Houk, K. N. *J. Org. Chem.* **2009**, *74*, 6944. (d) Cucinotta, C. S.; Kosa, M.; Melchiorre, P.; Cavalli, A.; Gervasio, F. L. *Chem.—Eur. J.* **2009**, *15*, 7913. (e) Cook, T. C.; Andrus, M. B.; Ess, D. H. *Org. Lett.* **2012**, *14*, 5836. (f) Sengupta, A.; Sunoj, R. B. *J. Org. Chem.* **2012**, *77*, 10525. (g) Zhu, J.-L.; Zhang, Y.; Liu, C.; Zheng, A.-M.; Wang, W. *J. Org. Chem.* **2012**, *77*, 9813. For a review: (h) Marcelli, T. *WIREs Comput. Mol. Sci.* **2011**, *1*, 142.

(18) (a) Li, X.; Deng, H.; Zhang, B.; Li, J. Y.; Zhang, L.; Luo, S. Z.; Cheng, J. -P. *Chem.—Eur. J.* **2010**, *16*, 450. (b) Xue, X. S.; Yu, A.; Cai, Y.; Cheng, J. -P. *Org. Lett.* **2011**, *13*, 6054. (c) Li, X.; Xue, X. S.; Liu, C.; Wang, B.; Tan, B. X.; Jin, J. L.; Zhang, Y.-Y.; Dong, N.; Cheng, J. -P. *Org. Biomol. Chem.* **2012**, *10*, 413. (d) Li, X.; Zhang, Y.-Y.; Xue, X. S.; Jin, J.-L.; Tan, B.-X.; Liu, C.; Dong, N.; Cheng, J.-P. *Eur. J. Org. Chem.* **2012**, 1774.

(19) (a) Johnson, E. R.; Keinan, S.; Mori-Sanchez, P.; Contreras-Garcia, J.; Cohen, A. J.; Yang, W. T. *J. Am. Chem. Soc.* **2010**, *132*, 6498. (b) Contreras-Garcia, J.; Johnson, E. R.; Keinan, S.; Chaudret, R.; Piquemal, J. P.; Beratan, D. N.; Yang, W. T. *J. Chem. Theory Comput.* **2011**, *7*, 625.

(20) For a recent review on weak hydrogen bonds: Takahashi, O.; Kohno, Y.; Nishio, M. *Chem. Rev.* **2010**, *110*, 6049.

(21) For examples (a) Washington, Y.; Houk, K. N. *Angew. Chem., Int. Ed.* **2001**, *40*, 4485. (b) Cannizzaro, C. E.; Houk, K. N. *J. Am. Chem. Soc.* **2002**, *124*, 7163. (c) Bahmanyar, S.; Houk, K. N.; Martin, H. J.; List, B. *J. Am. Chem. Soc.* **2003**, *125*, 2475. (d) Krenske, E. H.; Houk, K. N. *Acc. Chem. Res.* **2013**, *46*, 979.

(22) (a) Taylor, M. S.; Jacobsen, E. N. *Angew. Chem., Int. Ed.* **2006**, *45*, 1520. (b) Yu, X.; Wang, W. *Chem. Asian. J.* **2008**, *3*, 516. (c) Connon, S. J. *Chem. Commun.* **2008**, 2499. (d) Wang, Y.; Deng, L. *In Catalytic Asymmetric Synthesis*; Ojima, I., Ed.; ; Wiley-VCH: Weinheim, Germany, 2010, pp 59−94. (e) Quigley, C.; Rodríguez Docampo, Z.; Connon, S. J. *Chem. Commun.* **2012**, *48*, 1443.

(23) (a) Zhao, Y.; Schultz, N. E.; Truhlar, D. G. *J. Chem. Phys.* **2005**, *123*, 161103. (b) Zhao, Y.; Schultz, N. E.; Truhlar, D. G. *J. Chem. Theory Comput.* **2006**, *2*, 364. (c) Zhao, Y.; Truhlar, D. G. *J. Chem. Theory Comput.* **2006**, *2*, 1009. (d) Zhao, Y.; Truhlar, D. G. *Theo. Chem. Acc.* **2008**, *120*, 215. (e) Zhao, Y.; Truhlar, D. G. *Chem. Acc. Res.* **2008**, *41*, 157. (f) Zhao, Y.; Truhlar, D. G. *Chem. Phys. Lett.* **2011**, *502*, 1.

(24) (a) Marenich, A. V.; Cramer, C. J.; Truhlar, D. G. *J. Phys. Chem. B* **2009**, *113*, 6378. (b) Ribeiro, R. F.; Marenich, A. V.; Cramer, C. J.; Truhlar, D. G. *J. Phys. Chem. B.* **2011**, *115*, 14556.

(25) (a) Schwabe, T.; Grimme, S. *Phys. Chem. Chem. Phys.* **2007**, *9*, 3397. (b) Schwabe, T.; Grimme, S. *Acc. Chem. Res.* **2008**, *41*, 569.

(26) Frisch, M. J.; et al. *Gaussian 09*, revision B.01; Gaussian, Inc.: Wallingford, CT, 2009.

(27) (a) Legault, C. Y. *CYLview*, 1.0b; Université de Sherbrooke: Sherbrooke (Québec) Canada , 2009; http://www.cylview.org. (b) Humphrey, W.; Dalke, A.; Schulten, K. *J. Mol. Graphics* **1996**, *14*, 33.

(28) A comprehensive conformational study for catalyst and transition states was performed (as referee suggested). The detailed description and the relevant data were summarized in Supporting Information (see Part A) for the clarity and concision of the manuscript.

(29) Wittkopp, A.; Schreiner, P. R. *Chem.—Eur. J.* **2003**, *9*, 407.

(30) Gomez-Bengoa, E.; Linden, A.; López, R.; Mugica-Mendiola, I.; Oiarbide, M.; Palomo, C. *J. Am. Chem. Soc.* **2008**, *130*, 7955.

(31) The unexpectedly high dissociation energy of **CP2a** is found to have no experimental or theoretical precedent in literature. It is only the finding of this computation by using three different methods which led to the same conclusion.

(32) Meot-Ner, M. *Chem. Rev.* **2005**, *105*, 213.

(33) (a) Mason, S. F. *J. Chem. Soc.* **1957**, 5010. (b) Mason, S. F.; Philip, J.; Smith, B. E. *J. Chem. Soc. A* **1968**, 3051. (c) Poizat, O.; Bardez, E.; Buntinx, G.; Alain, V. *J. Phys. Chem. A* **2004**, *108*, 1873.

(34) Solntsev, K. M.; Clower, C. E.; Tolbert, L. M.; Huppert, D. *J. Am. Chem. Soc.* **2005**, *127*, 8534.

(35) It should be pointed out that other tautomeric form of **QD-1a** might also exist, but **QD-1a′** should be the most important one. (See Scheme S4 for other possible tautomers of **QD-1a**).

(36) An additional transition state structure **TS2ee′** corresponding to proton H7″ moving from C6″ (**CP2e**) to C4″ (**CP2e′**) in Scenario III was located (Figure S14) according to one reviewer's suggestion. However, the **TS2ee′** was found to be only 1.8 kcal/mol higher than **CP2e**, indicating that this process would be very facile. For the comparison of the three mechanistic pathways, it was given in Figure S14 instead of in Figures 4 and 5. Please see SI for details.

(37) Knowles, R. R.; Jacobsen, E. N. *Proc. Natl. Acad. Sci. U.S.A.* **2010**, *107*, 20678.

(38) Lu, T.; Chen, F. W. *J. Comput. Chem.* **2012**, *33*, 580.

(39) For selected examples (a) Krenske, E. H.; Houk, K. N.; Harmata, M. *Org. Lett.* **2010**, *12*, 444. (b) Antoline, J. E.; Krenske, E.

H.; Lohse, A. G.; Houk, K. N.; Hsung, R. P. *J. Am. Chem. Soc.* **2011**, *133*, 14443.
(40) (a) Bader, R. F. W. *Acc. Chem. Res.* **1985**, *18*, 9. (b) Bader, R. F. W. *Chem. Rev.* **1991**, *91*, 893. (c) *Quantum Theory of Atoms in Molecules: Recent Progress in Theory and Application*; Matta, C., Boyd, R. J., Eds.; Wiley-VCH: New York, 2007.
(41) Grabowski, S. J. *Chem. Rev.* **2011**, *111*, 2597 and references cited herein..
(42) Espinosa, E.; Molins, E.; Lecomte, C. *Chem. Phys. Lett.* **1998**, *285*, 170.
(43) (a) Noyori, R. *Asymmetric Catalysis in Organic Synthesis*, John Wiley; New York, 1994. (b) Ojima, I. *Catalytic Asymmetric Synthesis*, 2nd ed.; John Wiley: New York, 2004.